Potential Cancer Chemopreventive in Vitro Activities of Monomeric Xanthone Derivatives from the Marine Algicolous Fungus *Monodictys putredinis*[#]

Anja Krick,[†] Stefan Kehraus,[†] Clarissa Gerhäuser,[‡] Karin Klimo,[‡] Martin Nieger,[§] Armin Maier,[||] Heinz-Herbert Fiebig,[||] Iuliana Atodiresei,[⊥] Gerhard Raabe,[⊥] Jörg Fleischhauer,[⊥] and Gabriele M. König*[,†]

Institute for Pharmaceutical Biology, University of Bonn, Nussallee 6, D-53115 Bonn, Germany, Division of Toxicology and Cancer Risk Factors, DKFZ−German Cancer Research Center, Im Neuenheimer Feld 280, D-69120 Heidelberg, Germany, Department of Inorganic Chemistry, University of Bonn, Gerhard Domagk Strasse 1, D-53121 Bonn, Germany, Institute for Organic Chemistry, RWTH Aachen, Landoltweg 1, D-52074 Aachen, Germany, and Oncotest GmbH, Institute of Experimental Oncology, Am Flughafen 12-14, D-79108 Freiburg, Germany

Received October 13, 2006

Investigation of the fungal strain *Monodictys putredinis* isolated from the inner tissue of a marine green alga led to the isolation of four new monomeric xanthones and a benzophenone. All structures were elucidated by extensive spectroscopic measurements. The relative configuration of compound **1** was determined by X-ray crystal structure analysis, while for **2** and **3** configurations were confirmed by NOE experiments. Absolute configurations for compounds **1**−**3** were deduced by comparing experimental circular dichroism spectroscopic data with those calculated employing quantum-chemical time-dependent density functional theory (TDDFT). The compounds were examined for their cancer chemopreventive potential. Xanthone **2** was shown to inhibit cytochrome P450 1A activity with an IC_{50} value of 3.0 μM. Compounds **2** and **3** displayed moderate activity as inducers of NAD(P)H:quinone reductase (QR) in cultured mouse Hepa 1c1c7 cells, with CD values (concentration required to double the specific activity of QR) of 12.0 and 12.8 μM, respectively. Compound **3** showed weak inhibition of aromatase activity.

Cancer chemoprevention aims to halt or reverse the development and progression of cancer cells through use of suitable nutrients and/or pharmacological agents that can interrupt cancer development at various steps during the initiation, promotion, or progression stages.[1,2] Modulation of enzymes involved in metabolic activation and excretion of carcinogens is one of the best investigated mechanisms of chemopreventive agents.[3] Phase 1 enzymes (cytochromes P450) activate xenobiotics by addition of functional groups that render these compounds more water soluble. Although phase 1 functionalization is required for complete detoxification, induction of phase 1 enzymes might increase the risk to produce ultimate carcinogens capable of reacting with DNA and initiating carcinogenesis. On the other hand, phase 2 enzymes conjugate the activated compounds to endogenous ligands such as glutathione (GSH) and glucuronic, acetic, or sulfuric acids, thus facilitating their excretion in the form of these conjugates. NAD(P)H:quinone reductase (QR) contributes to detoxification by the two-electron reduction of quinones to hydroquinones, which are then excreted in the form of their conjugation products. Generally, inhibition of (induced) phase 1 enzyme activity concomitantly with induction of phase 2 enzyme expression is considered a logical strategy in chemoprevention, which is especially beneficial during the initiation stage of carcinogenesis.

Tumor promotion is regarded typically as the second step of carcinogenesis.[4] Although cellular changes acquired during tumor promotion are reversible, repeated contact of initiated cells with tumor promotors finally leads to irreversible tumor progression. Tumor promotion is mediated by exogenous tumor promotors (e.g, chemicals or radiation), but an excess of endogenous factors including reactive oxygen species, and mediators of inflammation and hormones, also contribute to tumor promotion.[4,5] Therefore, the overproduction of reactive oxygen species as well as enzymes such as the cyclooxygenases, the key enzymes in prostaglandin biosynthesis, and aromatase, catalyzing the conversion of androgens into estrogens, are targets of chemoprevention.

Herein we describe the identification and structure elucidation of a series of monomeric xanthones, which were subsequently tested in a series of in vitro bioassays relevant for the inhibition of carcinogenesis in vivo to determine their cancer chemopreventive potential. Xanthone derivatives are an important group of natural products due to their multiple biological activities. In a recent review,[6] Pinto et al. have summarized enzyme and cellular systems influenced by xanthone derivatives, including aromatase, cyclooxygenases, and prostaglandin receptors, glutathione *S*-transferase, and quinone reductase, as well as various kinases and proteases. Further, they have reviewed numerous antimicrobial effects of xanthone derivatives and highlighted antitumor activity as well as antimutagenic and potential cancer chemopreventive properties of xanthones.[6] Lesch and Bräse described the xanthone structure as a so-called "privileged structure", since members of this structural class are able to interact with different types of drug targets.[7]

The genus *Monodictys* is rarely chemically explored and belongs to the ascomycetes. To date, only one paper dealing with natural products from *Monodictys* has been published. In 1999, Krohn et al. reported stemphytriol, a new member of the octahydroperylene stemphyl- and altertoxins, from the endophytic fungus *M. fluctuata*.[8] A culture of the fungus *Monodictys putredinis* was isolated from a marine green alga collected in Tenerife, Spain (September 1995).[9] In the present work, the *M. putredinis* strain was mass cultivated on a solid biomalt medium. LC-MS analysis indicated the presence of several interesting compounds in the ethyl acetate extract. VLC and HPLC separations resulted in the isolation of four new monomeric xanthones and a benzophenone (**1**−**5**).

[#] Dedicated to the late Dr. Kenneth L. Rinehart of the University of Illinois at Urbana−Champaign for his pioneering work on bioactive natural products.

* To whom correspondence should be addressed. Tel: +49228733747. Fax: +49228733250. E-mail: g.koenig@uni-bonn.de.

[†] Institute for Pharmaceutical Biology, University of Bonn.

[‡] German Cancer Research Center, Heidelberg.

[§] Department of Inorganic Chemistry, University of Bonn.

[⊥] University of Aachen.

[||] Oncotest GmbH Freiburg.

10.1021/np060505o CCC: $37.00
Published on Web 02/10/2007

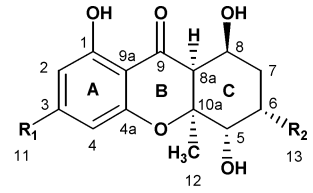

1 Monodictysin A
$R_1 = CH_3$, $R_2 = OH$

2 Monodictysin B
$R_1 = H$, $R_2 = CH_3$

3 Monodictysin C
$R_1 = OCH_3$, $R_2 = CH_3$

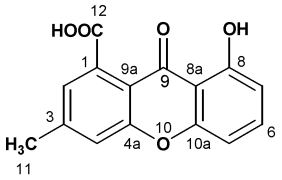

4 Monodictyxanthone

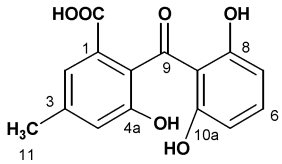

5 Monodictyphenone

Results and Discussion

The molecular formula of compound **1** was deduced by accurate mass measurement (HREIMS) to be $C_{15}H_{18}O_6$, implying seven degrees of unsaturation. The ^{13}C NMR spectrum contained 15 resonances resulting from two methyl, one methylene, six methine, and six quaternary carbons, including a carbonyl group (δ_C 201.4, C-9) (see Table 1). Three more elements of unsaturation were attributed to carbon−carbon double bonds of an aromatic moiety; thus the molecule had to be tricyclic. The direct connectivity (one bond) of proton and carbon atoms was deduced from a HSQC spectrum. Four ^1H NMR signals (δ_H 11.81, 4.14, 3.75, and 3.95) (see Table 1) were associated with hydroxyl groups due to missing HSQC cross-peaks. The downfield-shifted hydroxyl proton signal at δ_H 11.81 and an absorption in the IR spectrum at ν_{max} 1638 cm^{-1} indicated a hydrogen-bonded keto function in the β-position to a phenolic group (see Figure 1, fragment a). From the DEPT spectrum, 14 protons were evident, and together with four hydroxyl groups, the necessary number of 18 protons, as required by the molecular formula, was completed. Furthermore, with the presence of one carbonyl and four hydroxyl groups, one oxygen had to present as an ether linkage. ^{13}C NMR shift values of δ_C 75.1, 64.6, and 69.5 corresponded to oxygenated sp^3-hybridized methine groups. Two aromatic protons (δ_H 6.23, H-2 and 6.19, H-4) appeared as broad singlets in the ^1H NMR spectrum. Both of these showed $^1H-^1H$ COSY correlations (see Table 1) to a methyl group (δ_H 2.25, CH_3-11) to which both were adjacent, implying that H-2 and H-4 had to be in a *meta*-position to one another (see Figure 1, b). The ^1H NMR spectra and $^1H-^1H$ COSY correlations revealed a distinct $^1H-^1H$ spin system for protons H-5 to H-8a (see Figure 1, c). Due to the fact that three of the hydroxyl groups showed COSY cross-peaks, their position could be assigned and they were located in fragment c (C-5, C-6, and C-8). The second methyl group (δ_H 1.44, CH_3-12) appeared as a singlet in the ^1H NMR spectrum and showed no COSY correlations; a HMBC correlation to δ_C 82.7 indicated a position adjacent to the quaternary carbon C-10a and completed the fourth fragment of compound **1** shown in Figure 1, d. The connection of fragments a and b was deduced from HMBC correlations (H-2 to C-1, C-4, C-9a, C-11; H-4 to C-2, C-4a, C-9, C-9a, C-11; H_3-11 to C-2, C-3, C-4) and led to the construction of the aromatic ring A. The downfield carbon shift of C-4a (δ_C 160.6) revealed a second oxygenated sp^2-hybridized carbon additional to C-1. The HMBC correlations of the hydrogen-bonded phenolic hydroxyl group (OH-1) to C-1, C-2, and C-9a proved the linkage of keto group C-9 to C-9a and showed that H-2 is in *ortho*-position to C-1. HMBC correlations of the methyl group, H_3-12, to C-5, C-8a, and C-10a showed fragment d to be connected to C-5 and C-8a and thus completed the saturated six-membered ring C. This was supported by long-range correlations from H-5 to C-8a and C-10a. The chemical shifts of the quaternary carbon atoms C-10a (δ_C 82.7 ppm) and C-4a (δ_C 160.6 ppm) indicated a junction to an oxygen. With all hydroxyl groups being allocated, C-10a and C-4a had to be involved in the ether formation. Consistent with the chemical shift of the sp^3-hybridized methine group C-8a (δ_C 51.8), its linkage to the ketone group completed the third ring within **1**.

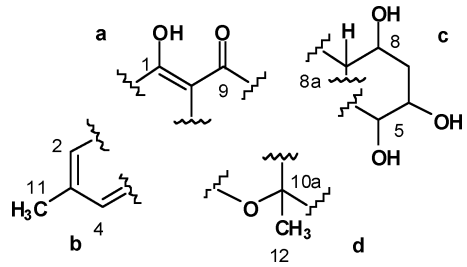

Figure 1. Fragments of compound **1** deduced from ^1H, $^1H-^1H$ COSY, and $^1H-^{13}C$ HMBC NMR spectra.

Table 1. 1D and 2D NMR Spectroscopic Data for Monodictysin A (**1**)

position	δ_C (mult.)[a]	δ_H (J in Hz)[b]	COSY[b,c]	HMBC[b,d]	NOESY[b,c]
1	162.4 (C)				
2	109.3 (CH)	6.23 (br s)	4, 11	1, 4, 9a, 11	11
3	150.3 (C)				
4	109.3 (CH)	6.19 (br s)	2, 11	2, 4a, 9, 9a, 11	11
4a	160.6 (C)				
5	75.1 (CH)	3.86 (br s)	OH−5, 6	6, 7, 8a, 10a, 12	6, 12
6	64.6 (CH)	4.46 (br d, 12.5)	5, OH−6, 7α/β		5, 7β
7	34.5 (CH_2)	2.02 (Hα td, 12.5, 3.0)	6, 7β, 8	5, 6	7β, 8, 8α
		1.86 (Hβ dt, 12.5, 3.6)	6, 7α, 8	5, 6, 8, 8a	6, 7α, 8
8	69.5 (CH)	4.35 (m)	7α/b, 8α, OH−8	6, 10a	7α/β, 8a
8a	51.8 (CH)	2.48 (br s)	8		8, 7α, 12
9	201.4 (C)				
9a	108.6 (C)				
10a	82.7 (C)				
11	22.3 (CH_3)	2.25 (br s)	2, 4	2, 3, 4	2, 4
12	22.9 (CH_3)	1.44 (s)		5, 8a, 10a	5, 8a
OH-1		11.81 (s)		1, 2, 9a	
OH-5		4.14 (br s)	5	10a	
OH-6		3.75 (br s)	6		
OH-8		3.95 (d, 5.5)	8		

[a] Acetone-d_6 300/75.5 MHz. [b]Acetone-d_6, 500/125.7 MHz. [c]Numbers refer to proton resonances. [d]Numbers refer to carbon resonances.

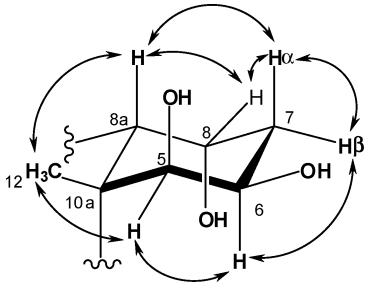

Figure 2. Selected NOESY correlations of ring C of compound **1**.

Compound **1** was thus identified as a tetrahydroxanthone. The systematic name according to IUPAC rules is 1,3,4,8-tetrahydroxy-4a,6-dimethyl-1,2,3,4,4a,9a-hexahydro-9*H*-xanthen-9-one. We propose the trivial name monodictysin A.

2D ^{1}H−^{1}H NOESY experiments and the analysis of ^{1}H−^{1}H coupling constants enabled the relative configuration of **1** to be deduced (see Figure 2). According to the observed NOESY cross-peaks between CH_3-12 and the proton at C-8a, the saturated ring C and ring B were *cis* connected. As H-8a showed a NOESY correlation to H-7α, both possessed an axial position. The axial position of H-7α was confirmed by $J_{H-6,H-7\alpha} = 12.5$ Hz, also indicating H-6 to have an axial orientation. The absence of other large ^{1}H−^{1}H coupling constants and the analysis of the remaining NOE correlations (see Table 1 and Figure 2) required equatorial orientations for H-5 and H-8. All assignments established a chair conformation for ring C. The relative configuration was therefore described as 5*R**, 6*R**, 8*R**, 8a*R**, and 10a*R**.

Recrystallization of xanthone **1** in acetone gave yellow crystals. X-ray studies confirmed the relative configuration found on the basis of NMR data. The absolute configuration could not be determined reliably [refinement of Flack's *x*-parameter: $x = 0.4(10)$].[10] Results are shown in Figures 3 and S10, Supporting Information. Compound **1** crystallized with two independent molecules and one solvent molecule (acetone) in the asymmetric unit.

Compound **2** had the molecular formula $C_{15}H_{18}O_5$, as deduced by accurate mass measurement. All general assumptions were the same as for compound **1**. Comparison of the ^{1}H and ^{13}C NMR spectra of **2** with those of **1** revealed that both compounds belong to the same structural type, but some differences could be observed. Instead of a signal for a quaternary carbon at δ_C 150.3 (C-3 in **1**) compound **2** possesses a sp^2-hybridized methine carbon (δ_C 138.3 and δ_H 7.33, CH-3). The signal of this aromatic proton appeared in the proton spectrum as a triplet, and the protons H-2 and H-4 as doublets, indicating all protons to be adjacent. In the ^{1}H NMR spectrum of **2** only three signals belonging to hydroxyl groups (δ_H 11.87, OH-1; 4.37, OH-5, 3.75, OH-8) were observed, and an additional methyl group (δ_H 1.03, d, $J = 7$ Hz, δ_C 18.1, CH_3-13) was visible (see Table 2). The ^{1}H−^{1}H COSY spectrum showed a linkage from CH_3-13 to CH-6 (δ_H 2.56 and δ_C 26.2). Additionally, in a HMBC experiment the protons of the methyl group CH_3-13 (δ_H 1.03) exhibited cross-peaks to C-5, C-6, and C-7. All these assignments were consistent with the methyl group CH_3-13 being positioned at C-6. Thus, compound **2** is a hydroxanthone like compound **1**, but the substitution pattern at C-3 and C-6 is different. We propose the trivial name monodictysin B.

For compound **3**, the molecular formula, $C_{16}H_{20}O_6$, was deduced by HREIMS analysis. All spectroscopic data were very similar to those of compound **2**. In the ^{1}H NMR spectrum one signal for an aromatic proton was missing, but an additional signal for a methoxyl group (CH_3-11) was observed. A HMBC correlation of H_3-11 to C-3 (δ_C 168.4) enabled location of the methoxyl group at C-3 (see Table 3). For compound **3** the trivial name monodictysin C is proposed.

Selective NOE measurements were undertaken to establish the relative configurations of compounds **2** and **3**. These measurements showed the same correlations as observed for compound **1** (see above). Therefore all three monomeric tetrahydroxanthones possess the same relative configuration as shown in Figure 2.

To determine the absolute configurations of **1**−**3**, circular dichroism (CD) measurements were combined with quantum-chemical calculations based on the time-dependent density functional theory. Geometry optimizations with the 6-31+G* basis set at the Hartree−Fock level were performed assuming the relative stereochemistry deduced from the NMR experiments and X-ray analysis (5*R**,6*R**,8*R**,8a*R**,10a*R**). The general shapes of the experimental CD spectra of xanthones **1**−**3** are quite similar (Figures 4A, and S6A and S7A, Supporting Information). They all show a strongly positive band at about 210 nm, followed by negative Cotton effects between 240 and 286 nm. The CD curves then change their signs at about 300 nm, leading to positive bands between 309 and 360 nm. The calculated CD spectra of xanthones **1**−**3** (Figure 4B and S6B, S7B) have strongly negative bands of almost equal intensity around 205 nm, followed by a weak positive Cotton effect at 232 nm for **1**, 230 nm for **2**, and 227 nm for **3** (for further discussion, see the Supporting Information). The CD spectra calculated for the 5*R*,6*R*,8*R*,8a*R*,10a*R* enantiomers of compounds **1**−**3** are close to the mirror images of the measured spectra (drawn

Table 2. 1D and 2D NMR Spectroscopic Data for Monodictysin B (**2**)[a]

position	δ_C (mult.)	δ_H (*J* in Hz)	COSY[b]	HMBC[c]	NOESY[b]
1	162.5 (C)				
2	108.5 (CH)	6.35 (d, 7.9)	3	4, 9a	
3	138.3 (CH)	7.33 (t, 7.9)	2, 4	1, 4a	
4	108.5 (CH)	6.32 (d, 7.9)	3	2, 4a, 9a	
4a	161.3 (C)				
5	75.4 (CH)	3.59 (br s)	OH−5	7, 8a, 10a, 12, 13	6, 12, 13
6	26.2 (CH)	2.56 (m)	7a, 13		5, 7*β*, 13
7	34.6 (CH_2)	1.82 (Hα td, 13.0, 2.4)	6, 7α, 8	6	7*β*, 8, 8a, 13
		1.48 (H*β* dt, 13.0, 2.8)	6, 7*β*, 8	5, 8, 8a	6, 7α, 8, 13
8	69.1 (CH)	4.23 (m)	7α/*β*, 8a, OH-8		7α/*β*, 8a
8a	52.0 (CH)	2.45 (d, 4.3)	8	8, 9	7α, 8, 12
9	202.8 (C)				
9a	110.8 (C)				
10a	81.9 (C)				
12	23.0 (CH_3)	1.35 (s)		5, 8a, 10a	5, 8a, 13
13	18.1 (CH_3)	1.03 (d, 7.0)	6	5, 6, 7	5, 6, 7α/*β*
OH-1		11.87 (s)		1, 2, 9a	
OH-5		4.37 (d, 5.8)	5		
OH-8		3.75 (d, 4.9)	8		

[a] Acetone-d_6, 500/125.7 MHz. [b]Numbers refer to proton resonances. [c]Numbers refer to carbon resonances.

Table 3. 1D and 2D NMR Spectroscopic Data for Monodictysin C (**3**)

position	δ_C (mult.)[a]	δ_H (*J* in Hz)[b]	COSY[b,c]	HMBC[b,d]	NOESY[b,c]
1	164.5 (C)				
2	94.5 (CH)	5.92 (d, 2.0)	4	1, 3, 4, 9a	
3	168.4 (C)				
4	94.8 (CH)	5.88 (d, 2.0)	2	2, 3, 4a, 9a	
4a	162.7 (C)				
5	75.5 (CH)	3.57 (d, 4.4)	OH-5	7, 8a, 10a, 12, 13	6, 12, 13
6	26.2 (CH)	2.53 (m)	7α, 13	13	5, 7*β*, 13
7	34.5 (CH_2)	1.81 (H α td, 13.2, 3.0)	6, 7*β*, 8	5, 6	6, 7*β*, 8, 8a, 13
		1.47 (H*β* dt, 13.2, 2.5)	6, 7α, 8	5, 6, 8a	6, 7α, 8, 13
8	68.8 (CH)	4.21 (m)	7*β*, 8a, OH-8	6, 10a	7α/*β*, 8a
8a	51.7 (CH)	2.37 (d, 4.4)	8	8, 9, 12	7α, 8, 12
9	200.2 (C)				
9a	105.7 (C)				
10a	82.1 (C)				
11	55.8 (CH_3)	3.80 (s)		3	
12	23.2 (CH_3)	1.37 (s)		5, 8a, 10a	5, 8a
13	18.1 (CH_3)	1.02 (d, 7.0)	6	5, 6, 7	5, 6, 7α/*β*
OH-1		12.22 (s)		1, 2, 9a	
OH-5		4.39 (d, 5.8)	5		
OH-8		3.75 (d, 5.1)	8		

[a] Acetone-d_6, 300/75.5 MHz. [b] Acetone-d_6, 500/125.7 MHz. [c] Numbers refer to proton resonances. [d] Numbers refer to carbon resonances.

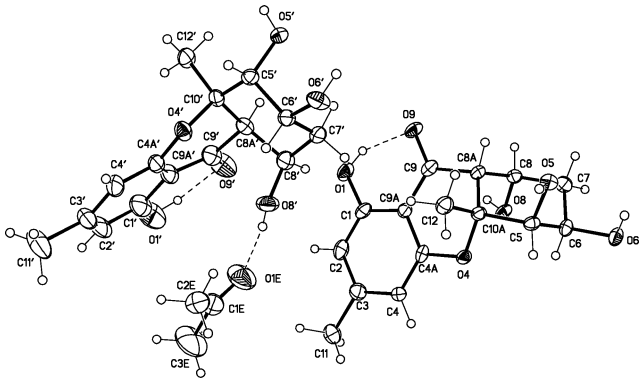

Figure 3. Asymmetric unit of **1** in the crystal. Displacement parameters are at the 50% probability level.

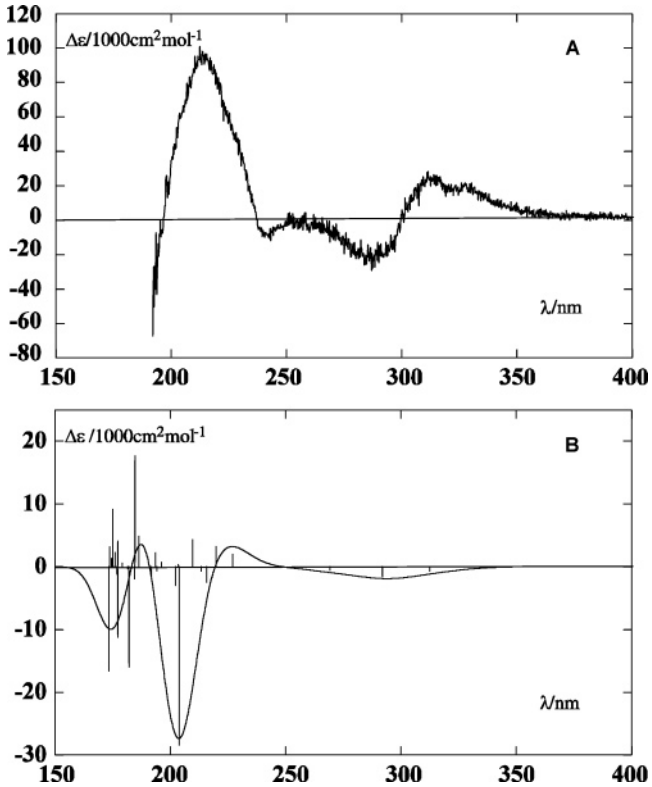

Figure 4. (A) Experimental CD spectrum of xanthone **3** recorded in methanol. (B) Calculated CD spectrum for the 5*R*,6*R*,8*R*,8a*R*,-10a*R* isomer of **3** at the B3LYP/TZVP//HF/6-31+G* level. The bars are $\Delta\epsilon_{max}$ of the single Gaussians and are proportional to the corresponding rotational strengths.

for compound **3** as an example in Figure 4). Therefore, the absolute configuration of the xanthones **1**−**3** is postulated as 5*S*,6*S*,8*S*,8a*S*,-10a*S*.

The molecular formula of compound **4** was analyzed by HREIMS to be $C_{15}H_{10}O_5$, with 11 degrees of unsaturation. The UV spectrum of the yellow powder showed four maxima (231, 254, 287, and 361 nm), suggesting a xanthone chromophore. Signals for 15 carbon atoms observed in the ^{13}C NMR spectrum resulted from one methyl group, five aromatic methine groups, and nine quaternary carbon atoms. The chemical shifts of all methine and quaternary carbons (>105 ppm) indicated them to be sp^2-hybridized, including one carbonyl (δ_C 181.9, C-9) and one carboxyl function (δ_C 169.8, C-12) (see Table 4). The IR absorption at 1698 cm^{-1} suggested a carboxyl function present as a carboxylic acid. ^{13}C NMR signals for 12 carbons resulted from two aromatic rings, and thus the tricyclic xanthone nucleus could be confirmed. Since eight protons were observed in the DEPT spectrum and thus directly connected to carbon atoms, and one hydrogen was present in the carboxyl group, the remaining proton was present as a hydroxyl group. ^1H NMR spectra showed five resonances for aromatic protons, one methyl group, and one hydrogen-bonded hydroxyl group (δ_H 12.37, OH-8). The chemical shift of δ_H 12.37 indicated a *β*-position to a carbonyl function. Three aromatic protons (C-5 to C-7) had to be *ortho*-positioned on one aromatic moiety due to their multiplicities (δ_H 7.01, d; 7.71, t; 6.79, d, all $J = 8.0$ Hz) and HMBC correlations. Long-range HMBC correlations of OH-8 (δ_H 12.37) to signals at δ_C 111.3 (C-7), 109.5 (C-8a), and 162.4 (C-8) showed CH-7 to reside next to C-8, with C-8a being connected to the carbonyl, C-9. Correlations from H-5 and H-6 to δ_C 156.8 completed the aromatic ring C with C-10a (δ_C 156.8) as the bridgehead carbon. The downfield ^{13}C NMR shift of C-10a was in agreement with an oxygenated carbon. Two aromatic protons ($\delta_{H/C}$ 7.26/125.2, CH-2, $\delta_{H/C}$ 7.48/119.5, CH-4) appeared as doublets ($^4J = 1.2$ Hz) in the ^1H NMR spectrum and thus had to be *meta*-positioned to each other. $^1H-^1H$ COSY and HMBC cross-peaks showed their *ortho*-position to the methyl group CH_3-11 ($\delta_{H/C}$ 2.52/21.8), which was bonded to C-3 (δ_C 148.7). The ^{13}C NMR shift of C-1 (δ_C 135.7) indicated the bonding to the carboxylic acid function (COOH-12). The resonances of H-2 revealed long-range correlations to δ_C 169.8 (COOH-12), 21.8 (CH_3-11), and 119.5 (CH-4) and the quarternary carbon C-9a (δ_C 115.5). The H-4 signal showed also a HMBC

Table 4. 1D and 2D NMR Spectroscopic Data for **4** and **5**

	monodictyxanthone (**4**)			monodictyphenone (**5**)		
position	δ_C (mult.)[a]	δ_H (*J* in Hz)[b]	HMBC[b,d]	δ_C (mult.)[a]	δ_H (*J* in Hz)[b]	HMBC[b,d]
1	135.7 (C)			129.6 (C)		
2	125.2 (CH)	7.26 (d, 1.2)	4, 9a, 11, 12	122.4 (CH)	7.34 (s)	4, 4a, 9, 11, 12
3	148.7 (C)			139.5 (C)		
4	119.5 (CH)	7.48 (d, 1.2)	2, 4a, 9, 9a, 11	121.1 (CH)	6.93 (s)	2, 4a, 9, 9a, 11
4a	157.2 (C)			154.1 (C)		
5	107.9 (CH)	7.01 (d, 8.0)	8a, 9, 10a	108.0 (CH)*	6.32* (d, 8.0)	6, 7, 8a, 8/10a, 9
6	138.1 (CH)	7.71 (t, 8.0)	8, 10a	136.6 (CH)	7.20 (t, 8.0)	5, 7, 8a, 8/10a
7	111.3 (CH)	6.79 (d, 8.0)	5, 8, 8a	108.0 (CH)*	6.32* (d, 8.0)	5, 6, 8a, 8/10a, 9
8	162.4 (C)			162.9 (C)**		
8a	109.5 (C)			112.6 (C)		
9	181.9 (C)			202.1 (C)		
9a	115.5 (C)			131.9 (C)		
10a	156.8 (C)			162.9 (C)**		
11	21.8 (CH_3)	2.52 (s)	1, 2, 3, 4	21.1 (CH_3)	2.31 (s)	1, 2, 3, 4, 4a, 9, 9a
12	169.8 (C)			167.5 (C)		
OH-8		12.37 (br s)	7, 8a, 8			

[a] Acetone-d_6, 300/75.5 MHz. [b]Acetone-d_6, 500/125.7 MHz. [c]Numbers refer to proton resonances. [d]Numbers refer to carbon resonances, * and ** interchangeable signals due to chemical equivalence.

correlation to C-9a, revealing a *meta*-position to C-2 and C-4. HMBC correlation of H-4 to C-4a (δ_C 157.2) allowed the conclusion that C-4a completed ring A. The carbon shift of δ_C 157.2 was in agreement with a connection to an oxygen being the ether bridge to the other aromatic moiety. Compound **4** is a new trisubstituted xanthone with the systematic name 8-hydroxy-3-methyl-9-oxo-9*H*-xanthene-1-carboxylic acid. We propose the trivial name monodictyxanthone.

Compound **5** exhibited a molecular formula of $C_{15}H_{12}O_6$, as deduced by accurate mass measurement, implying 10 degrees of unsaturation. Compared to compound **4**, **5** was lacking one degree of unsaturation and showed a mass difference of 18 mass units (H_2O). The similarity to compound **4** was obvious in all of the NMR data (see Table 4), and the same substitution patterns for the aromatic rings were concluded for both compounds. The molecule of **2** possesses, however, three hydroxyl groups and was only bicyclic. The UV spectrum of compound **5** missed a third maximum typical of xanthone UV spectra but had only two absorption maxima (λ_{max} 206 and 276 nm), being in agreement with an aromatic molecule. In compound **5**, NMR resonances for C-8 and C-10a (δ_C 162.9) and for H-5 and H-7 (δ_H 6.32) were identical, i.e., magnetically equivalent. This observation is in accordance with a symmetrically substituted aromatic ring C possessing free hydroxyl groups at C-8 as well as C-10a. The third hydroxyl group of **5** was positioned at C-4a (δ_C 154.1). Thus, compound **5** possesses a bicyclic benzophenone structure in the same manner as deduced for xanthone **4**. According to IUPAC rules, the name of compound **5** is 2-(2,6-dihydroxybenzoyl)-3-hydroxy-5-methylbenzoic acid. Monodictyphenone is proposed as the trivial name for **5**.

Compounds **1** to **3** are structurally related to diversonol[11] and α- and β-diversonolic esters,[12] fungal metabolites of *Penicillium diversum*. Additionally, hydroxanthones are known as part of the dimeric ergochromes and secalonic acids, respectively.[13] Monodictyxanthone (**4**) is related to several xanthones, possessing a carboxyl function at C-1, such as vertixanthones,[14] mycoxanthone,[14] and pinselic acid,[13] which are all fungal metabolites, and to cassiaxanthone[15] isolated from leaves of *Cassia* species. The benzophenone structure of compound **5** is structurally related to sulochrin[13] and balanol.[16]

All xanthone derivatives isolated during this study may result from an octaketide-based precursor via an anthraquinone skeleton.[17−19] In contrast to the well-investigated secalonic acids, which all possess a methyl group at C-6, the hydroxanthone structures **1**−**3** show varying positions for their methyl groups. These are either at C-3 or at C-6 and may result from cleavage of the anthraquinone skeleton either between C-4a or C-10a and carbonyl C-10 (see biogenetic scheme, Figure S10, Supporting Information).

Table 5. Influence of **1**−**5** on Carcinogen-Metabolizing Enzymes

	Cyp1A inhibition	NAD(P)H:quinone reductase induction (QR)	
compound	IC_{50} (μM)[a]	CD (μM)[b]	IC_{50} (μM)[a]
1	>50 (40)	191.1[c]	>400
2	23.3 ± 3.9	12.0 ± 4.8	>50
3	3.0 ± 0.7	12.8 ± 2.6	>50
4	34.8 ± 7.4	>50 (1.4)	>50
5	>50 (28)	>50 (1.3)	>50

[a] IC_{50}: half-maximal inhibitory concentration. Values in parentheses indicate the percentage of inhibition at the indicated concentration.[b]CD: concentration required to double the specific activity of QR. Values in parentheses indicate the maximum fold induction at the indicated concentration. [c]The compound was tested at least three times at increasing concentrations to reach the CD value.

Secalonic acids result from a cleavage between C-4a and C-10. The fungus *Monodictys putredinis* seems to be capable of both enzymatic reactions. Moreover, xanthones **1**−**3** are substituted with a methyl group at C-10a, whereas all secalonic acids and other recently isolated dimeric xanthones (xanthochinodines,[20] neosartorin,[21] rugulotrosins[22]) possess a carboxylic acid methyl ester at this position. Phomoxanthones[23] and dicerandrols[24] are substituted with a hydroxymethyl moiety at C-10a. To date, only diversonol is known as a hydroxanthone structure with a completely reduced carbonyl function at C-10a.[11,25]

The xanthones were tested in a series of bioassays indicative of potential cancer chemopreventive activities. First, we analyzed their potential to modulate drug-metabolizing enzymes, i.e., inhibition of the phase I enzyme Cyp1A and induction of the phase II enzyme NAD(P)H:quinone reductase (QR). These mechanisms are most relevant during the initiation phase of carcinogenesis, when the interaction of activated carcinogens with DNA might result in DNA damage and mutations if not repaired. Cyp1A is involved in the activation of polyaromatic hydrocarbons like benzo[*a*]pyrene, of aflatoxin B1, and of cooked food mutagens including IQ, Glu-P1, and PhIP.[26] Xanthone **3**, substituted with a methoxyl group at C-3 of ring A, was identified as the most potent Cyp1A inhibitor and inhibited the β-naphthoflavone-induced enzymatic activity of H4IIE cell homogenates in a dose-dependent fashion with a half-maximal inhibitory concentration (IC_{50}) of 3.0 ± 0.7 μM (Table 5 and Figure 5A). Lack of the methoxyl group at C-3 in compound **2** reduced the inhibitory potential by about 7.7-fold, whereas compound **1**, substituted with a methyl group in C-3 position and a hydroxyl group in C-6 position, inhibited the enzyme activity by only 40% at a final test concentration of 50 μM. The xanthone-carboxylic acid **4** showed dose-dependent Cyp1A activity inhibition with an

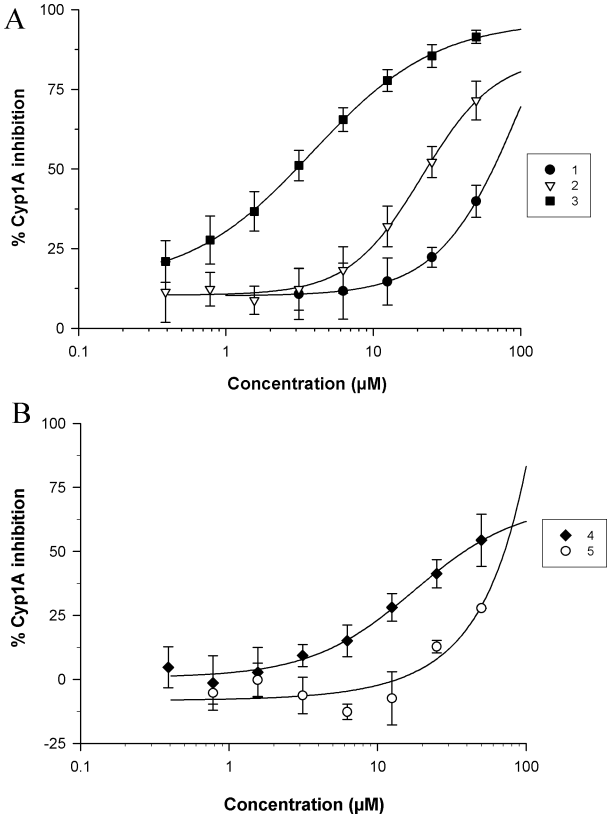

Figure 5. Dose-dependent inhibition of Cyp1A enzymatic activity by the hydroxyxanthones **1**, **2**, and **3**, respectively (A), in comparison with the inhibitory potential of compounds **4** and **5** (B). Cyp1A activity was measured with β-naphthoflavone-induced H4IIE rat hepatoma cell homogenates by dealkylation of 3-cyano-7-ethoxycoumarin to fluorescent 3-cyano-7-hydroxycoumarin. Activities of β-naphthoflavone-induced controls were in the range 48.5−137.7 nmol/min/mg of protein ($n = 13$). α-Naphthoflavone used as a positive control inhibited Cyp1A activity with an IC_{50} value of 0.0035 ± 0.0009 μM.

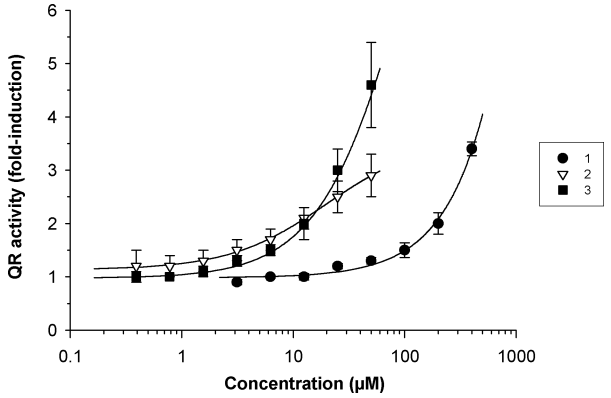

Figure 6. Induction of QR activity in Hepa 1c1c7 cell culture by compounds **1**, **2**, and **3**. The specific QR activity of untreated controls was 43 ± 10 nmol/min/mg protein ($n = 7$). β-Naphthoflavone was used as a positive control and induced QR activity with a CD value of 0.146 ± 0.063 μM.

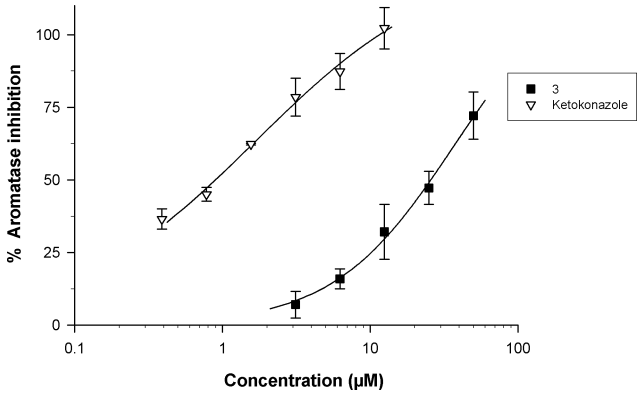

Figure 7. Dose-dependent inhibition of aromatase activity by the xanthone **3** in comparison with ketokonazole used as a positive control substance with an IC_{50} value of 0.9 ± 0.1 μM. Aromatase activity was measured using human recombinant aromatase (human Cyp 19 + P450 reductase supersomes) and *O*-benzylfluorescein benzyl ester as a substrate.

IC_{50} value of 34.8 ± 7.4 μM. In contrast, opening of ring B, resulting in the bicyclic benzophenone **5**, significantly reduced the inhibitory potential (28% inhibition at a test concentration of 50 μM, summarized in Table 5 and Figure 5B).

We further monitored the induction of NAD(P)H:quinone reductase (QR) as a model phase 2 enzyme in Hepa 1c1c7 murine hepatoma cell culture. The hydroxanthones **1**−**3** were found to induce QR specific activity in a dose-dependent manner (Figure 6). Compounds **2** and **3** were identified as the most potent inducers, with CD values of 12.0 ± 4.8 and 12.8 ± 2.6 μM, without demonstrating cytotoxic effects at concentrations up to 50 μM (Table 5). For compound **1**, a CD value of 191.1 μM was determined. The compound was tested at concentrations up to 400 μM without any signs of cytotoxicity.

Compounds **4** and **5** did not induce QR activity >2-fold up to a concentration of 50 μM. Due to limited compound availability, we were not able to increase the final concentration tested. Activation of carcinogens might lead to the generation of reactive radicals. Consequently, we determined radical-scavenging potential of compounds **1**−**5** using the stable radical 1,1-diphenyl-2-picrylhydrazyl (DPPH).[27] None of the compounds demonstrated DPPH-scavenging potential when tested at concentrations up to 250 μM. Antioxidant potential was investigated by scavenging of superoxide anion radicals generated by oxidation of hypoxanthine to uric acid by xanthine oxidase.[27] Up to concentrations of 50 μM, none of the compounds were identified as a superoxide anion scavenger. We further determined oxygen radical absorbance capacity (ORAC), using 2,2-azobis(2-amidinopropane) dihydrochloride (AAPH) as a peroxyl-radical generator.[28] At a concentration of 1 μM, none of the compounds were more potent in scavenging peroxyl radicals than the water-soluble vitamin E analogue Trolox, used as a reference compound.

For the detection of antitumor-promoting potential, the influence of compounds **1**−**5** was evaluated on cyclooxygenase-1 (COX-1) and aromatase enzymatic activities.[27,29,30] None of the compounds inhibited COX-1 activity more than 50% at a concentration of 100 μM; therefore, IC_{50} values were not generated. Interestingly, xanthone **3**, identified as the most potent Cyp1A inhibitor, also inhibited the activity of aromatase with an IC_{50} value of 28.3 ± 4.5 μM in a dose-dependent manner (Figure 7), whereas compounds **1**, **2**, **4**, and **5** were less inhibitory, with a maximum 32, 9, 37, and 25% inhibition, respectively, at a test concentration of 50 μM.

In summary, the monomeric xanthones **1**−**3** were identified as inhibitors of the Cyp1A isoenzyme, which is involved in the metabolic conversion of procarcinogens into carcinogens. Compounds **2** and **3** displayed moderate activity as inducers of QR, a carcinogen-detoxifying enzyme, and compound **3** was identified as a weak inhibitor of aromatase activity essential for the biosynthesis of estrogens. Overall, the substitution pattern of the core structure strongly influenced the biological effects.

Experimental Section

General Experimental Procedures. Optical rotations were measured on a JASCO DIP 140 polarimeter. UV and IR spectra were obtained employing Perkin-Elmer Lambda 40 and Perkin-Elmer

Spectrum BX instruments, respectively. ^{1}H (1D, 2D COSY) and ^{13}C (1D, DEPT 135, 2D HSQC, 2D HMBC) NMR spectra were recorded on Bruker Avance 500 DRX and Bruker Avance 300 DPX spectrometers in acetone-d_6. Spectra were referenced to residual solvent signals with resonances at $\delta_{H/C}$ 2.04/28.9 (acetone-d_6). HREIMS were recorded on a Finnigan-MAT 95 spectrometer. HPLC-MS measurements were recorded employing an Agilent 1100 Series HPLC including DAD, with a reversed-phase C_{18} column (Macherey-Nagel Nucleodur 100, 125 mm × 2 mm, 5 μm) and gradient elution (from MeOH−H_2O, 10:90, in 20 min to 100% MeOH, then isocratic for 10 min), coupled with an API 2000, Triple Quadrupole, LC/MS/MS, Applied Biosystems/MDS Sciex, and ESI source. Preparative HPLC was carried out using a Merck−Hitachi system consisting of a L-6200A pump, a L-4500 photodiode array detector, a D-6000 interface or a Waters system with 515 HPLC pump, and a Knauer K-2300 differential refractometer as detector.

Origin of the Algal Sample. The fresh algal sample was collected in September 1995 in Tenerife, Spain.[9] Until examination the sample was stored in sterile artificial seawater [ASW (g/L): KBr (0.1), NaCl (23.48), $MgCl_2 \times H_2O$ (10.61), $CaCl_2 \times 2\ H_2O$ (1.47), KCl (0.66), $SrCl_2 \times 6\ H_2O$ (0.04), Na_2SO_4 (3.92), $NaHCO_3$ (0.19), H_3BO_3 (0.03)]. Algal samples were rinsed three times with sterile water. After surface sterilization with 70% EtOH for 15 s the alga was rinsed in sterile ASW. The alga was aseptically cut into small pieces and placed on agar plates containing isolation medium: 15 g/L agar (Fluka Chemie GmbH, Buchs, Switzerland), ASW 800 mL/L, glucose 1 g/L, peptone from soymeal 0.5 g/L, yeast extract 0.1 g/L, benzyl penicillin 250 mg/L, and streptomycin sulfate 250 mg/L. A fungus found to grow out of the algal tissue was separated on biomalt medium (biomalt 20 g/L, agar 10 g/L, ASW 1000 mL/L) until the culture was pure. The fungal strain 187/195 15 I was identified as *Monodictys putredinis* (Wallroth) S. Hughes 1958 by Dr. R. A. Samson, Centralbureau voor Schimmelcultures, Utrecht, The Netherlands.

Cultivation. The fungal strain *M. putredinis* (strain number 187/195 15 I, culture collection of Institute for Pharmaceutical Biology, University of Bonn, Germany) was cultivated on 5 L (20 Fernbach flasks) of solid biomalt medium containing 50 g/L Biomalt (Villa Natura Gesundheitsprodukte GmbH, Kirn, Germany), 0.1 g/L yeast extract, and 15 g/L agar at room temperature for 4 months. Each Fernbach flask was inoculated with a piece of fungal biomass (1 cm^2) dissolved in 10 mL of sterile water.

Extraction and Isolation. Fungal biomass and media were diluted with water (100 mL/L) and homogenized using an Ultra-Turrax apparatus. Exhaustive extraction with 21 L of ethyl acetate (EtOAc) in three steps yielded 5.3 g of brown, oily extract. This was fractionated by normal-phase (NP) VLC (silica gel 60, 0.063−0.200 mm) using gradient elution from petroleum ether (PE), to EtOAc, acetone, and MeOH, to yield 11 fractions. Fraction 4 showed interesting ^{1}H NMR spectra and antimicrobial activity; the LC-MS fingerprint chromatogram contained several interesting peaks. Fraktion 4 was separated by NP HPLC (column Knauer Si Eurospher-100, 250 × 8 mm, 5 μm, PE−acetone 7.5:2.5, 2 mL/min) to yield 11 fractions. Five fractions were purified by RP HPLC (Knauer C_{18} Eurospher-100 column, 250 × 8 mm, 5 μm, 2 mL/min) to yield seven pure compounds. Fraction 4.1 yielded 4.4 mg of compound **2** and 2.0 mg of furan-2-carboxylic acid. Fraction 4.3 gave 8.3 mg of compound **4** (RP18 MeOH−H_2O, 7:3). Fraction 4.6 was purified with H_2O−MeOH gradient elution to give 8.9 mg of compound **5**. Two other fractions were purified with an isocratic solvent composition of MeOH−H_2O (80:20) to yield 8.8 mg of compound **3**, 4.0 mg of acetyl Sumiki's acid, and 6.0 mg of compound **1**. Workup of fraction 5 led to reisolation of xanthones **1**−**4**, whereas an additional 210 mg of monodictysin A (**1**) was isolated as the main compound in this fungal extract.

Monodictysin A, (1*S*,3*S*,4*S*,4a,9a*S*)-1,3,4,8-tetrahydroxy-4a,6-dimethyl-1,2,3,4,4a,9a-hexahydro-9*H*-xanthen-9-one (1): white-brown solid (216 mg, 43.2 mg/L); $[\alpha]^{24}_D$ +53 (*c* 0.43 $CHCl_3$); UV (MeOH) λ_{max} (log ϵ) 209 (4.05), 282 (3.79), 351 (3.19) nm; IR (ATR) ν_{max} 3392, 1638, 1203, 1100, 750 cm^{-1}; ^{1}H and ^{13}C NMR data (see Table 1); ESIMS *m*/*z* 295 [M + H$^+$], 293 [M − H$^+$]; EIMS *m*/*z* 294 (90), 191 (88), 151 (100); HREIMS *m*/*z* 294.1109 (calcd for $C_{15}H_{18}O_6$ 294.1103).

Monodictysin B, (1S,3S,4S,4aS,9aS)-1,4,8-trihydroxy-3,4a-dimethyl-1,2,3,4,4a,9a-hexahydro-9*H*-xanthen-9-one (2): white solid (13.3 mg, 2.7 mg/L); $[\alpha]^{24}_D$ +80.5 (*c* 0.20 $CHCl_3$); UV (MeOH) λ_{max} (log ϵ) 207 (4.19), 276 (3.87), 353 (3.38) nm; IR (ATR) ν_{max} 3459, 3364, 1626, 1461 cm^{-1}; ^{1}H and ^{13}C NMR data (see Table 2); ESIMS *m*/*z* 279 [M + H$^+$], 277 [M − H$^+$]; EIMS *m*/*z* 278 (50), 177 (95), 137 (98); HREIMS *m*/*z* 278.1153 (calcd for $C_{15}H_{18}O_5$ 278.1154).

Monodictysin C, (1S,3S,4S,4aS,9aS)-1,4,8-trihydroxy-6-methoxy-3,4a-dimethyl-1,2,3,4,4a,9a-hexahydro-9*H*-xanthen-9-one (3): white solid (22.5 mg, 4.5 mg/L); $[\alpha]^{24}_D$ +102 (*c* 0.50 $CHCl_3$); UV (MeOH) λ_{max} (log ϵ) 215 nm (4.19), 292 nm (4.07), 331 nm (3.34); IR (ATR) ν_{max} 3445, 1636, 1458, 1158 cm^{-1}; ^{1}H and ^{13}C NMR data (see Table 3); ESIMS *m*/*z* 309 [M + H$^+$], 307 [M − H$^+$]; EIMS *m*/*z* 308 (41), 207 (100); HREIMS *m*/*z* 308.1262 (calcd for $C_{16}H_{20}O_6$ 308.1260).

Monodictyxanthone, 8-hydroxy-3-methyl-9-oxo-9*H*-xanthene-1-carboxylic acid (4): yellow solid (12.0 mg, 2.4 mg/L); UV (MeOH) λ_{max} (log ϵ) 231 nm (4.13), 254 nm (4.05), 287 (3.69), 361 (3.38) nm; IR (ATR) ν_{max} 2921, 2851, 1698, 1645, 1605, 1272, 1237, 820 cm^{-1}; ^{1}H and ^{13}C NMR data (see Table 4); ESIMS *m*/*z* 271 [M + H$^+$], 269 [M − H$^+$]; EIMS *m*/*z* 270 (62), 252 (85), 226 (73); HREIMS *m*/*z* 270.0530 (calcd for $C_{15}H_{10}O_5$ 270.0528).

Monodictyphenone, 2-(2,6-dihydroxybenzoyl)-3-hydroxy-5-methylbenzoic acid (5): yellow solid (8.9 mg, 3.6 mg/L); UV (MeOH) λ_{max} (log ϵ) 206 (4.56), 276 (4.02) nm; IR (ATR) ν_{max} 3258, 1692, 1613, 1452, 1224, 759 cm^{-1}; ^{1}H and ^{13}C NMR data (see Table 4); ESIMS *m*/*z* 306 [M + NH_4^+], 287 [M − H$^+$]; EIMS *m*/*z* 288 (5), 270 (100), 252 (51), 226 (45); HREIMS *m*/*z* 288.0636 (calcd for $C_{15}H_{12}O_6$ 288.0634).

Furan-2-carboxylic acid and acetyl Sumiki's acid: identified by comparison of ^{1}H, ^{13}C NMR and ESIMS data.[31,32]

Biological Assays. Compounds **1**−**5** were tested in agar diffusion assays against different bacteria, fungi, and a green microalga.[9] Cytotoxicity of the compounds **1**−**5** was investigated using six tumor cell lines,[33] in addition to a reporter gene assay, protein phosphatase assay, Hsc70 ATPase assay, and β-secretase inhibition.[34] The pure compounds showed no activity in these assays.

Determination of Potential Cancer Chemopreventive Activities. Experimental details of most test systems utilized in this study are summarized in Gerhauser et al.[27,35] Briefly, inhibition of Cyp1A (EC 1.14.14.1) enzymatic activity and induction of QR (EC 1.6.99.2) in cultured Hepa1c1c7 cells were assayed as described by Crespi et al. (1997) and Gerhauser et al. (1997), monitoring the dealkylation of 3-cyano-7-ethoxycoumarin to 3-cyano-7-hydroxycoumarin and the NADPH-dependent menadiol-mediated reduction of MTT [3-(4,5-dimethylthiazo-2-yl)-2,5-diphenyltetrazolium bromide] to a blue formazan, respectively.[36,37] Radical-scavenging potential was determined photometrically by reaction with 1,1-diphenyl-2-picrylhydrazyl (DPPH) free radicals in a microplate format.[27] Oxygen radical absorbance capacity using fluorescein and AAPH as a peroxyl radical generator was quantified as described by Huang et al. (2002).[28] Inhibition of COX-1 (prostaglandin G/H synthase, EC 1.14.99.1) activity was determined with a modification of the system described by Jang et al. (1997), measuring oxygen consumption during the conversion of arachidonic acid to prostaglandins.[29] Inhibition of aromatase activity was estimated using human recombinant Cyp19 (EC 1.14.14.1) and *O*-benzylfluorescein benzyl ester (DBF) as a substrate.[30]

Crystal Structure Determination of 1. Data were collected on a Nonius KappaCCD diffractometer at −150 °C using Mo Kα radiation (λ = 0.71073 Å). The structures were solved by direct methods (SHELXS-97).[38] Non-hydrogen atoms were refined anisotropically and H atoms with a riding model (H(O) free) on F^2 (full-matrix least-squares, SHELXL-97).[39] The absolute configuration could not be determined reliably by refinement of Flack's *x*-parameter [*x* = 0.4(10)].[10] Compound **1**: yellow crystals from acetone, $C_{15}H_{18}O_6$ 0.5 acetone, M = 323.33, crystal size 0.40 × 0.15 × 0.05 mm, orthorhombic, space group $P2_12_12_1$ (No. 19); a = 7.4702(1) Å, b = 9.1258(2) Å, c = 46.9743(11) Å, V = 3202.31(11) Å^3, Z = 8, ρ(calcd) = 1.341 Mg m^{-3}, $F(000)$ = 1376, μ = 0.103 mm^{-1}, 9288 reflections measured, 4789 unique reflections [R_{int} = 0.029] used for structure solution and refinement with 443 parameters and 8 restraints, R_1 (for 3766 $I > 2\sigma(I)$) = 0.0370, wR_2 = 0.0797 (all data), largest difference peak and hole 0.650 and −0.167 e Å^{-3}. Crystallographic data for the structure reported in this paper have been deposited with the Cambridge Crystallographic Data Centre (CCDC-604188). Copies of the data can be obtained, free of charge, on application to the Director, CCDC, 12 Union Road, Cambridge CB2 1EZ, UK (fax: +44-(0)1223-336033 or e-mail: deposit@ccdc.cam.ac.uk).

Circular Dichroism Spectroscopic Measurement. CD spectra of **1**−**3** were recorded at room temperature in methanol on an AVIV 62DS CD spectrometer. The concentration and the path length was 1.5×10^{-3} mol/L and 0.05 cm for all three samples.

Computational Methods. All calculations were performed with the GAUSSIAN03 package of quantum-chemical programs running on the facilities of the computing center of the RWTH Aachen.[40] CD spectra for the 5*R*,6*R*,8*R*,8a*R*,10a*R* isomers of **1**−**3** were calculated by means of the quantum-chemical time-dependent density functional theory (TDDFT).[41] Optimizations at the Hartree−Fock level employing the 6-31+G* basis set were performed to obtain molecular geometries to be used in the calculation of the CD spectra. To define starting geometries, we used the information from the determination of the solid structure of **1** which confirmed the conclusions drawn from the NMR study. The rotational strengths required to calculate the CD spectra have been obtained in TDDFT calculations with the B3LYP functional,[42] a TZVP (triple ζ for valence orbitals plus polarization functions) basis set,[43] and the origin-independent dipole-velocity formalism.[44]

Acknowledgment. We thank Dr. G. Eckhardt, Institute for Organic Chemistry, University of Bonn, Germany, for recording the EIMS. For financial support we thank the Bundesministerium für Bildung und Forschung (BMBF), research program 03F0415A.

Supporting Information Available: ^{1}H and ^{13}C NMR spectra of xanthones **1**−**5**, electronic transitions and rotational strengths for the 10 lowest excited states of xanthones **1**−**3**, experimental and calculated CD spectra of xanthones **1** and **2**, optimized structures of xanthones **1**−**3** (HF/6-31+G* level), further discussion of CD spectra, and biogenetic scheme for compounds **1**−**5**. This material is available free of charge via the Internet at http://pubs.acs.org.

References and Notes

(1) Kelloff, G. J.; Boone, C. W.; Steele, V. E.; Crowell, J. A.; Lubet, R. A.; Greenwald, P.; Hawk, E. T.; Fay, J. R.; Sigman, C. C. *IARC Sci. Publ.* **1996**, *139*, 203−219.
(2) Greenwald, P. *Toxicology* **2001**, *166*, 37−45.
(3) Talalay, P.; Fahey, J. W.; Holtzclaw, W. D.; Prestera, T.; Zhang, Y. *Toxicol. Lett.* **1995**, 82−83, 173−179.
(4) Trosko, E. *Nutr. Cancer* **2006**, *54*, 102−110.
(5) Reid, S. E.; Murthy, M. S.; Kaufman, M.; Scanlon, E. F. *Br. J. Surg.* **1996**, *83*, 1037−1046.
(6) Pinto, M. M.; Sousa, M. E.; Nascimento, M. S. *Curr. Med. Chem.* **2005**, *12*, 2517−2538.
(7) Lesch, B.; Bräse, S. *Angew. Chem., Int. Ed.* **2004**, *43*, 115−118.
(8) Krohn, K.; John, M.; Aust, H. J., Schulz, B. *Nat. Prod. Lett.* **1999**, *14*, 31−34.
(9) Höller, U. Isolation, biological activity and secondary metabolite investigations of marine-derived fungi and selected host sponges. Ph.D. Thesis, University of Braunschweig, Germany 1999.
(10) Flack, H. D. *Acta Crystallogr.* **1983**, *A39*, 876−881.
(11) Turner, W. B. *J. Chem. Soc., Perkin Trans. 1* **1978**, 1621.
(12) Holker, J. S. E.; O'Brien, E.; Simpson, T. J. *J. Chem. Soc., Perkin Trans. 1* **1983**, *7*, 1365−1368.
(13) Turner, W. *Fungal Metabolites*; Academic Press: London, 1971; pp 169−173.
(14) Ayer, W. A.; Browne, L. M.; Lin, G. *J. Nat. Prod.* **1989**, *52*, 119−129.
(15) Nair, M. S. R.; McMorris, T. C.; Anchel, M. *Phytochemistry* **1970**, *9*, 1153−1155.
(16) Miyabe, H.; Torieda, M.; Inoue, K.; Tajiri, K.; Kiguchi, T.; Naito, T. *J. Org. Chem.* **1998**, *63*, 4397−4407.
(17) Franck, B.; Flasch, H. *Prog. Chem. Org. Nat. Prod.* **1973**, *30*, 151−206.
(18) Steyn, P. S. *J. Environ. Pathol. Toxicol. Oncol.* **1992**, *11*, 47−59.
(19) Kurobane, I.; Vining, L. C., McInnes, A. G. *J. Antibiot.* **1979**, *32*, 1256−1266.
(20) Tabata, N.; Tomoda, H.; Iwai, Y.; Omura, S. *J. Antibiot.* 1**996**, *49*, 267−271.
(21) Proksa, B.; Uhrin, D.; Liptaj, T.; Sturdikova, M. *Phytochemistry* **1998**, *48*, 1161−1164.
(22) Stewart, M.; Capon, R. J.; White, J. M.; Lacey, E.; Tennant, S.; Gill, J. H.; Shaddock, M. P. *J. Nat. Prod.* **2004**, *67*, 728−730.
(23) Isaka, M.; Jaturapat, A.; Rukseree, K.; Danwisetkanjana, K.; Tanticharoen, M.; Thebtaranonth, Y. *J. Nat. Prod.* **2001**, *64*, 1015−1018.
(24) Wagenaar, M. M.; Clardy, J. *J. Nat. Prod.* **2001**, *64*, 1006−1009.
(25) Nising, C. F.; Ohnemuller, U. K.; Bräse, S. *Angew. Chem., Int. Ed.* **2006**, *45*, 307−309.
(26) Lewis, D. F.; Lake, B. G. *Xenobiotica* **1996**, *26*, 723−753.
(27) Gerhauser, C.; Klimo, K.; Heiss, E.; Neumann, I.; Gamal-Eldeen, A.; Knauft, J.; Liu, G. Y.; Sitthimonchai, S.; Frank, N. *Mutat. Res.* **2003**, *523*−*524*, 163−172.
(28) Huang, D.; Ou, B.; Hampsch-Woodill, M.; Flanagan, J. A.; Prior, R. L. *J. Agric. Food Chem.* **2002**, *50*, 4437−4444.
(29) Jang, M.; Cai, L.; Udeani, G. O.; Slowing, K. V.; Thomas, C. F.; Beecher, C. W.; Fong, H. H.; Farnsworth, N. R.; Kinghorn, A. D.; Metha, R. G.; Moon, R. C.; Pezzuto, J. M. *Science* **1997**, *275*, 218−220.
(30) Stresser, D. M.; Turner, S. D.; McNamara, J.; Stocker, P.; Miller, V. P.; Crespi, C. L.; Patten, C. J. *Anal. Biochem.* **2000**, *284*, 427−430.
(31) Corey, E. J.; Slomp, G.; Dev, S.; Tobinga, S.; Glazier, E. R. *J. Am. Chem. Soc.* **1958**, *80*, 1204−1206.
(32) Jadulco, R.; Proksch, P.; Wray, V.; Sudarsono, A. B.; Gräfe, U. *J. Nat. Prod.* **2001**, *64*, 527−530.
(33) Dengler, W. A.; Schulte, J.; Berger, D. P.; Mertelsmann, R.; Fiebig, H. H. *Anticancer Drugs* **1995**, *6*, 522−532.
(34) Mueller, D. Biosynthetic potential of cyanobacteria: Isolation of bioactive peptides from the cyanobacterium *Tychonema* sp. Ph.D. Thesis, University of Bonn, Germany 2006.
(35) Gerhauser, C.; Alt, A.; Heiss, E.; Gamal-Eldeen, A.; Klimo, K.; Knauft, J.; Neumann, I.; Scherf, H. R.; Frank, N.; Bartsch, H.; Becker, H. *Mol. Cancer Ther.* **2002**, *1*, 959−969.
(36) Gerhauser, C.; You, M.; Liu, J.; Moriarty, R. M.; Hawthorne, M.; Mehta, R. G.; Moon, R. C.; Pezzuto, J. M. *Cancer Res.* **1997**, *57*, 272−278.
(37) Crespi, C. L.; Miller, V. P.; Penman, B. W. *Anal. Biochem.* **1997**, *248*, 188−190.
(38) Sheldrick, G. M. *Acta Crystallogr.* **1990**, *A46*, 467−473.
(39) Sheldrick, G. M. *SHELXL-97*, Program for crystal structure refinement; University of Göttingen: Germany, 1997.
(40) Frisch, M. J.; Trucks, G. W.; Schlegel, H. B.; Scuseria, G. E.; Robb, M. A.; Cheeseman, J. R.; Montgomery, J. A., Jr.; Vreven, T.; Kudin, K. N.; Burant, J. C.; Millam, J. M.; Iyengar, S. S.; Tomasi, J.; Barone, V.; Mennucci, B.; Cossi, M.; Scalmani, G.; Rega, N.; Petersson, G. A.; Nakatsuji, H.; Hada, M.; Ehara M.; Toyota, K.; Fukuda, R.; Hasegawa, J.; Ishida, M.; Nakajima, T.; Honda, Y.; Kitao, O.; Nakai, H.; Klene, M.; Li, X.; Knox, J. E.; Hratchian, H. P.; Cross, J. B.; Adamo, C.; Jaramillo, J.; Gomperts, R.; Stratmann, R. E.; Yazyev, O.; Austin, A. J.; Cammi, R.; Pomelli, C.; Ochterski, J. W.; Ayala, P. Y.; Morokuma, K.; Voth, G. A.; Salvador, P.; Dannenberg, J. J.; Zakrzewski, V. G.; Dapprich, S.; Daniels, A. D.; Strain, M. C.; Farkas, O.; Malick, D. K.; Rabuck, A. D.; Raghavachari, K.; Foresman, J. B.; Ortiz, J. V.; Cui, Q.; Baboul, A. G.; Clifford, S.; Cioslowski, J.; Stefanov, B. B.; Liu, G.; Liashenko, A.; Piskorz, P.; Komaromi, I.; Martin, R. L.; Fox, D. J.; Keith, T.; Al Laham, M. A.; Peng, C. Y.; Nanayakkara, A.; Challacombe, M.; Gill, P. M. W.; Johnson, B.; Chen, W.; Wong, M. W.; Gonzalez, C.; Pople, J. A. *Gaussian 03*, Revision C.02; Gaussian, Inc.: Wallingford, CT, 2004.
(41) Bauernschmidt, R.; Ahlrichs, R. *J. Chem. Phys.* **1996**, *256*, 454−464.
(42) (a) Lee, C.; Yang, W.; Parr, R. G. *Phys. Rev. B* **1988**, *37*, 785−789. (b) Miehlich, B.; Savin, A.; Stoll, H.; Preuss, H. *Chem. Phys. Lett.* **1989**, *157*, 200−206. (c) Becke, A. D. *J. Chem. Phys.* **1993**, *98*, 5648−5652.
(43) Schäfer, A.; Huber, C.; Ahlrichs, R. *J. Chem. Phys.* **1994**, *100*, 5289−5835.
(44) Moscowitz, A. In *Modern Quantum Chemistry*; Sinanoglu, O., Ed.; John Wiley & Sons, Inc.: New York, 1965; Vol. 3, p 21ff.

NP060505O